Anthocyanidins Inhibit Epithelial–Mesenchymal Transition Through a TGF-β/Smad2 Signaling Pathway in Glioblastoma Cells

Amira Ouanouki, Sylvie Lamy, and Borhane Annabi*

Laboratoire d'Oncologie Moléculaire, Centre de Recherche BioMed, Université du Québec à Montréal, Montréal, Québec, Canada

Epidemiological studies have convincingly demonstrated that diets rich in fruits and vegetables play an important role in preventing cancer due to their polyphenol content. Among polyphenols, the anthocyanidins are known to possess anti-inflammatory, cardioprotective, anti-angiogenic, and anti-carcinogenic properties. Despite the well-known role of transforming growth factor-β (TGF-β) in high grade gliomas, the impact of anthocyanidins on TGF-β-induced epithelial–mesenchymal transition (EMT), a process that allows benign tumor cells to infiltrate surrounding tissues, remains poorly understood. The objective of this study is to investigate the impact of anthocyanidins such as cyanidin (Cy), delphinidin (Dp), malvidin (Mv), pelargonidin (Pg), and petunidin (Pt) on TGF-β-induced EMT and to determine the mechanism(s) underlying such action. Human U-87 glioblastoma (U-87 MG) cells were treated with anthocyanidins prior to, along with or following the addition of TGF-β. We found that anthocyanidins differently affected TGF-β-induced EMT, depending on the treatment conditions. Dp was the most potent EMT inhibitor through its inhibitory effect on the TGF-β Smad and non-Smad signaling pathways. These effects altered expression of the EMT mesenchymal markers fibronectin and Snail, as well as markedly reducing U-87 MG cell migration. Our study highlights a new action of anthocyanidins against EMT that supports their beneficial health and chemopreventive effects in dietary-based strategies against cancer.

Key words: anthocyanidins; chemoprevention; EMT; glioblastoma; Smad2; TGF-β

INTRODUCTION

Glioblastoma multiforme (GBM) is the most common aggressive brain cancer [1]. Patients with GBM have a median survival time of less than 15 months even with an aggressive therapy consisting of a combined tumor resection, irradiation, and temozolomide administration [2,3]. Despite advances in our understanding of tumor biology, the invasiveness that characterizes GBM makes it resistant to standard treatments [4,5]. Therefore, better understanding of the mechanisms that promote cancer cell progression in GBM are of great clinical importance.

Carcinoma invasion is driven by a cellular process called epithelial–mesenchymal transition (EMT) [6]. EMT was first described as a distinct cell differentiation process in the late 70s, but has received increasing attention since it not only occurs in embryonic development but also contributes to pathological conditions [7]. During EMT, epithelial cells lose epithelial markers such as the adherens junction proteins E-cadherin and cytokeratin, and acquire mesenchymal markers including N-cadherin, fibronectin, vimentin, and some soluble metalloproteinases [8]. Consequently, epithelial cells lose their polarity (apical-basal) and undergo changes in morphology and cytoskeletal organization, generating mesenchymal-like cells with increased migratory properties [8]. EMT can be induced by several growth factors produced by tumor-associated stroma, such as heparin-binding growth factor, hepatocyte growth factor, epidermal growth factor, platelet-derived growth factor, and transforming growth factor β (TGF-β) [9]. TGF-β is known to act as a tumor suppressor in normal tissues as well as a tumor promoter during tumorigenesis [10]. This growth factor represents the most potent inducer of EMT through the activation of types I and II serine-threonine kinase receptors, TbRI and TbRII, which activate receptor-regulated Smads (R-Smads) [11]. The activated R-Smads form complexes with co-Smads, translocate to the nucleus and regulate EMT target

Abbreviations: Cy, cyanidin; Dp, delphinidin; EMT, epithelial–mesenchymal transition; ERK, extracellular signal-regulated kinase; GBM, glioblastoma multiforme; JNK, c-Jun N-terminal kinase; JNK/Stat3, janus kinase/signal transducer and activator of transcription 3; Mv, malvidin; Pg, pelargonidin; Pt, petunidin; R-Smad, receptor-regulated Smad; TGF-β, transforming growth factor-beta.

Conflict of interest: The authors have no conflicts of interest to declare.

Grant sponsor: Institutional Research Chair in Cancer Prevention and Treatment

*Correspondence to: Laboratoire d'Oncologie Moléculaire, Université du Québec à Montréal, C.P. 8888, Succ. Centre-ville, Montréal, Québec, Canada H3C 3P8.

Received 13 May 2016; Revised 1 September 2016; Accepted 16 September 2016

DOI 10.1002/mc.22575

Published online 4 October 2016 in Wiley Online Library (wileyonlinelibrary.com).

genes by interacting with various transcription factors (Snail, Slug, and Twist) [11]. Aside from the Smad signaling pathway, TGF-β also activates non-Smad signaling pathways such as extracellular signal-regulated kinase (ERK), c-Jun N-terminal kinase (JNK), and p38 MAP kinases, Rac1, RhoA, and Cdc42 GTPases [12]. Therefore, preventing EMT by affecting TGF-β signaling pathways may prove efficient in preventing tumor progression.

Approaches to preventing tumor progression can involve several different approaches, including changes to the patient's diet to include more foods derived from plants [13]. The cancer preventive effects of fruits and vegetables are widely supported by results from several in vitro, in vivo, and epidemiological studies [14–16]. This property has been mainly attributed to the presence of phytochemicals, such as polyphenols, which interfere with several processes involved in cancer and metastasis. A number of these polyphenols, for example, α-mangostin, curcumin, epigallocatechin gallate, resveratrol, and gallic acid, are known to target EMT [17].

Anthocyanidins, and their glycosylated forms the anthocyanins, are abundant flavonoids present in berries, red grapes, red cabbages, and other pigmented fruits and vegetables [18,19]. Consumption of anthocyanidins is known to lower the carcinogenic activity of multiple cancer cell types in vitro and tumor types in vivo [20]. These molecules have been shown to reduce cell proliferation, inflammation, angiogenesis, and invasion. It was reported that anthocyanins also modulate the expression of some genes involved in EMT processes, such as Snail, by inhibiting NF-κB or Akt signaling pathways [17,21]. Since the effects of anthocyanidins on EMT have never been studied, we have investigated whether molecules such as cyanidin (Cy), delphinidin (Dp), malvidin (Mv), pelargonidin (Pg), and petunidin (Pt) could abrogate TGF-β-induced EMT in U-87 glioblastoma (U-87 MG) cells.

MATERIALS AND METHODS

Materials

Anthocyanidin compounds Cy (purity ≥ 96%), Dp, Pg, Mv (purity ≥ 97%), and Pt (purity ≥ 95%) were purchased from Extrasynthese (Lyon, France). Recombinant human TGF-β1 was obtained from R&D Systems (Minneapolis, MN). Electrophoresis reagents were purchased from Bio-Rad (Mississauga, ON). The anti-ERK-1/2 (K-23) polyclonal antibody and the anti-Twist1 monoclonal antibody were from Santa Cruz Biotechnologies (Santa Cruz, CA). Antibodies against Snail, Slug, phospho-Smad2, Smad2, GAPDH (glyceraldehyde-3-phosphate dehydrogenase), and phospho-p44/42 MAPK were from Cell Signaling Technology (Beverly, MA). The anti-fibronectin antibody was from Sigma–Aldrich (Oakville, ON). Anti-mouse and anti-rabbit horseradish peroxidase (HRP)-linked secondary antibodies were purchased from Jackson ImmunoResearch Laboratories (West Grove, PA) and enhanced chemiluminescence (ECL) reagents were from Denville Scientific Inc. (Metuchen, NJ). Micro bicinchoninic acid protein assay reagents were from Thermo Scientific (Rockford, IL).

Cell Culture

The human U-87 MG cell line was purchased from American Type Culture Collection (Manassas, VA). Cells were maintained in Eagle's Minimum Essential Medium (Wisent, 320-036-CL) supplemented with 10% calf serum (HyClone Laboratories, SH30541.03), 1 mM sodium pyruvate (Sigma–Aldrich, P2256), 2 mM L-glutamine, 100 units/mL penicillin, and 100 mg/mL streptomycin (Wisent, 450-202-EL), and cultured at 37°C under a humidified 95–5% (v/v) mixture of air and CO_2. Cells were treated with vehicle (0.1% ethanol) or with anthocyanidins in the absence of serum prior to (pre-treatment), along with (co-treatment) or following (post-treatment) addition of 10 ng/mL TGF-β.

Western Blot Analysis

To study the expression of EMT markers during TGF-β treatment as well as the effect of anthocyanidins, TGF-β (10 ng/mL) and/or anthocyanidins were added to the cells as described below. U-87 MG cells were pre-treated with anthocyanidins for 24 h, followed by TGF-β for 48 h, or serum starved for 24 h and co-treated with anthocyanidins and TGF-β for 48 h, or serum starved for 24 h followed by the addition of TGF-β for 48 h and post-treated with anthocyanidins for the last 24 h. Cells were then washed with ice-cold phosphate-buffered saline (PBS) containing 1 mM each of sodium fluoride (NaF) and sodium orthovanadate (Na_3VO_4) and incubated in the same medium for 30 min at 4°C. The cells were solubilized in lysis buffer [150 mM NaCl, 10 mM Tris–HCl, pH 7.4, 1 mM EDTA, 1 mM ethyleneglycol-O, O′-bis(2-aminoethyl)-N, N, N′, N′-tetraacetic acid (EGTA), 0.5% (vol/vol) Nonidet P-40 and 1% (vol/vol) Triton X–100]. The resulting lysates were solubilized in Laemmli sample buffer [125 mM Tris–HCl (pH 6.8), 20% glycerol, 4% SDS, 10% β-mercaptoethanol, and 0.00125% bromophenol blue], boiled for 4 min, and separated by sodium dodecyl sulfate-polyacrylamide gel electrophoresis (SDS–PAGE). After electrophoresis, proteins (25 μg) were transferred to polyvinylidene difluoride (PVDF) membranes, which were then blocked 1 h at room temperature (RT) with 5% nonfat dry milk in Tris-buffered saline/Tween 20 (TBS-T; 147 mM NaCl, 20 mM Tris–HCl, pH 7.5, and 0.1% Tween 20). Membranes were further washed three times in TBS-T and incubated with the primary antibody in TBS-T containing 3% bovine serum albumin (BSA) and 0.01% sodium azide, followed by a 1 h incubation with HRP-conjugated anti-mouse or anti-rabbit antibodies in TBS-T containing 5% nonfat dry milk.

Immunoreactive material was visualized with an ECL detection system. The immunoreactive bands were quantified with ImageJ software (NIH).

Immunofluorescence

U-87 MG cells were seeded on cover slips and treated with ethanol (0.1%) or TGF-β (10 ng/mL) for 48 h. Cells were washed twice with cold PBS, fixed in 4% formaldehyde for 20 min at room temperature and permeabilized with 0.5 % Triton X–100 for 5 min. After three washes with ice-cold PBS for 15 min (total), non-specific binding was blocked with 1% BSA in PBS for 1 h at RT. Cells were then incubated with the primary antibody (anti-fibronectin or anti-Slug; 1:200) for 1 h at RT, washed twice with cold PBS and incubated with Alexa Fluor-488 conjugated anti-rabbit IgG (Invitrogen, Eugene, OR) at 1:200 for 1 h at RT. The cell nuclei were visualized with 1 μg/mL 4′, 6-diamidino-2-phenylindole (DAPI) staining for 5 min at RT. Slides were then dried, mounted with the ProLong Gold antifade reagent (FisherScientific, Ottawa, ON) and the fluorescence examined by microscopy.

Real-Time PCR Analysis

U-87 MG cells were incubated in 6-well plates for 48 h then TGF-β (10 ng/mL) was added for another 48 h. Following treatment, total RNA was isolated using TRIzol reagent (Life technologies, Gaithersburg, MD) and cDNA was synthesized using the high capacity cDNA reverse transcription kit (Applied Biosystems, Foster City, CA) according to the manufacturer's instructions. Quantitative PCR was performed using SsoFast EvaGreen Supermix (Bio-Rad, Hercules, CA). DNA amplification was carried out using a CFX Connect Real-Time System (Bio-Rad) and product detection was performed by measuring binding of the fluorescent dye EvaGreen to double stranded DNA. The QuantiTect primers sets were from Qiagen: Snail (Hs_SNAI1_1_SGQT00010010), fibronectin (Hs_FN1_1_SGQT00038024), Slug (Hs_SNAI2_1_SG QT00044128), Twist (Hs_TWIST1_1_SGQT00011956), GAPDH (Hs_GAPDH_2_SG QT01192646), and β-actin (Hs_Actb_2_SGQT01680476). The relative quantities of target gene mRNA compared against two internal controls, GAPDH and β-actin RNA, were measured by following a ΔCT method employing an amplification plot (fluorescence signal vs. cycle number). The difference (ΔC_T) between the mean values in the triplicate samples of target gene and that of GAPDH and β-actin mRNAs were calculated by CFX Manager software version 2.1 (Bio-Rad) and the relative quantified value (RQV) was expressed as $2^{-\ \Delta C_T}$.

Cell Viability Assay

U-87 MG cells were treated as described above with anthocyanidins alone. After 72 h of total treatment, cells were washed twice with ice-cold PBS and viability was evaluated by the incorporation of propidium iodide (0.5 μg/mL, BD Biosciences, Mississauga, ON) using the BD Accuri C6 flow cytometer. 10 000 cells per sample were counted, and the percentage of live and dead cells was evaluated using the BD CSampler software.

Real-Time Cell Migration Assay

Experiments were carried out using the Real-Time Cell Analyser (RTCA), Dual-Plate (DP) Instrument, and the xCELLigence system (Roche Diagnostics, Laval, QC), following the instructions of the supplier. The optimal seeding concentration of cells and TGF-β concentration for migration assay were first determined. U-87 MG cells were treated in pre-, co-, or post-treatment conditions with anthocyanidins (25 μM) ± TGF-β as described above. After a total treatment of 72 h, 250 000 cells per well were seeded in a CIM-plate 16 (Roche Diagnostics), and incubated at 37°C under a humidified atmosphere containing 5% CO_2 for 24 h. Prior to cell seeding, the underside of each well in the upper chamber was coated with 0.15% gelatin in PBS and incubated for 1 h at 37°C. The lower chamber was filled with serum-free medium. The upper chamber of each well was filled with 250 000 cells. After 30 min of adhesion, cell migration was monitored every 5 min for 24 h. The impedance value was measured by the RTCA DP Instrument and expressed as an arbitrary unit called the Cell Index. Each experiment was performed in quadruplicate wells.

Statistical Analysis

Statistical analyses were generally performed using one-way ANOVA with a post hoc Dunnett's test. Student's unpaired *t*-test was used to determine the statistical significance between the control and the stimulated control for the EMT markers. Differences with $P < 0.05$ were considered significant. All statistical analyses and graphs were performed using the GraphPad Prism software version 5.0b (San Diego, CA).

RESULTS

TGF-β Induces EMT in U-87 MG Cells

It has been reported that TGF-β plays an important role in GBM tumorigenesis [4,22]. In order to use the U-87 MG cell line as a model for epithelial–mesenchymal transition, we examined morphological changes as well as the expression levels of EMT markers such as fibronectin, Snail, Slug, and Twist by immunoblotting and quantitative PCR (Figure 1) after stimulation of U-87 MG cells with 10 ng/mL TGF-β for 48 h. In the absence of TGF-β, U-87 MG cells showed their standard morphology while, in the presence of TGF-β, U-87 MG cells adopted a more elongated, grouped and star-shaped mesenchymal-like morphology (Figure 1A). Western blot analysis showed that TGF-β increased the expression of the mesenchymal markers Slug, fibronectin, and Snail by 2.5-, 5-, and 220-fold, respectively

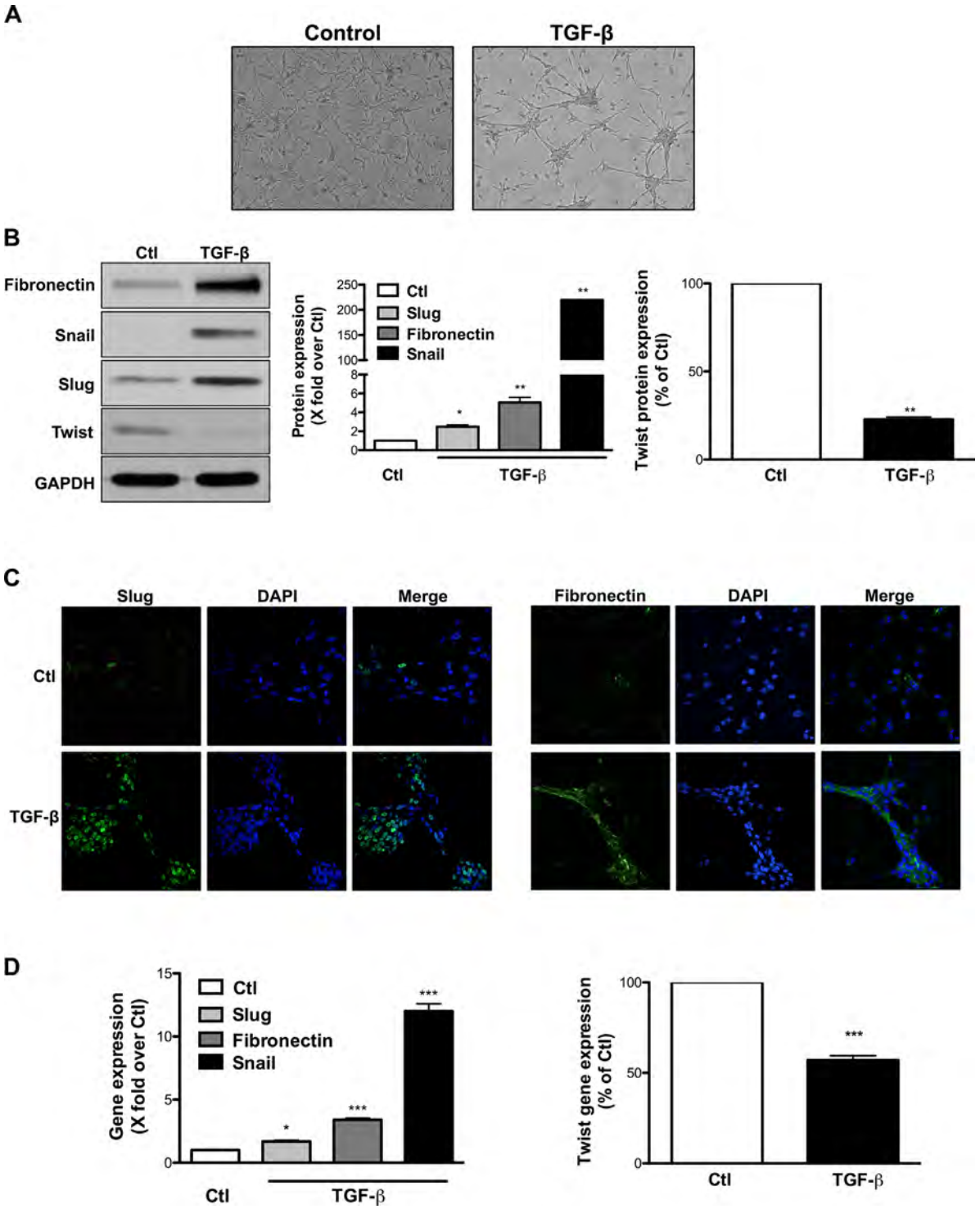

Figure 1. TGF-β-induced EMT in U-87 MG cells. U-87 MG cells were exposed to 10 ng/mL TGF-β for 48 h. (A) Cell morphology was compared between unstimulated and stimulated cells. (B) Western blot analysis demonstrated levels of protein expression for EMT markers fibronectin, Snail, Slug, and Twist. (C) Photomicrographs show the immunostaining of fibronectin (green), Slug (green), and nuclei (blue) using fluorescence microscopy. (D) The effect of TGF-β on EMT markers was evaluated by real-time PCR. Densitometric analysis is representative of three independent experiments. Statistically significant differences were calculated by unpaired Student's *t*-test (B) and one-way ANOVA followed by Dunnett's test (A, D) ($^{*}P < 0.05$, $^{**}P < 0.01$, and $^{***}P < 0.001$ vs. control cells).

(Figure 1B). Interestingly, we observed a 77% decrease in the expression of the transcription factor Twist. Two of these markers were analyzed by immunofluorescence and we found that TGF-β increased the nuclear translocation of Slug and the expression of the extracellular matrix protein fibronectin in the cytoplasm (Figure 1C). Finally, transcripts levels of the EMT markers were evaluated by real-time PCR which showed that TGF-β increased Slug, fibronectin, and Snail significantly (Figure 1D). As was seen for the protein level, the transcript levels of Twist decreased by 58% (Figure 1D). Taken together, these results indicate that TGF-β induced EMT in our U-87 MG cell model.

Pre-, Co-, and Post-Treatment With Anthocyanidins Affects the Expression of TGF-β-Induced EMT Markers

U-87 MG cells were incubated with serum-free medium, then pre-, co-, and post-treatments were performed with vehicle (0.1% ethanol) or 50 μM anthocyanidins for 24 h as described in the Materials and Methods section. After 48 h of stimulation with TGF-β, the expression of fibronectin, Snail, and Twist were determined using Western blot analysis (Figure 2). The TGF-β-induced Snail expression was inhibited by all five anthocyanidins tested in pre- (Figure 2A), co- (Figure 2B), and post-treatment (Figure 2C) with percentage inhibition ranging from 40% to 100%. Fibronectin expression was also down regulated by Dp via pre- and post-treatment by 92% and 60%, respectively (Fig. 2A,C), by Cy in co-treatment by 50% (Figure 2B) and by Mv in post-treatment by 45% (Figure 2C). However, the inhibition of Twist expression after TGF-β stimulation was not significantly reversed by the five anthocyanidins in either pre-, co-, or post-treatment at 50 μM. Overall, these results indicate that anthocyanidins can effectively reverse changes in the expression of selective mesenchymal markers such as Snail and fibronectin induced by TGF-β and appear to be effective whether used under pre-, co-, or post-treatment conditions.

Anthocyanidins Alter the Expression of TGF-β-Induced EMT Markers in a Dose-Dependent Manner

Prior to assessing different concentrations of anthocyanidins, we first determined whether these molecules were cytotoxic to U-87 MG cells (Table 1). Cell viability was evaluated by propidium iodide staining and flow cytometry. Since TGF-β alone did not change the viability of U-87 MG cells (data not shown), cells were incubated in serum-free medium in pre-, co-, and post-treatment with 35 μM or 50 μM of each anthocyanidin tested in the absence of TGF-β. Following these treatments, the percentage of living cells ranged from 90% to 100%, except for the pre-treatment with 50 μM Dp, which caused ~21 % of cells to die (Table 1).

To gain further insight into the inhibitory effects of anthocyanidins (Figure 2), we treated U-87 MG cells with various concentrations of anthocyanidins in order to determine the half-maximal inhibition concentrations (IC_{50}) values on the expression of TGF-β-induced EMT markers (Figure 3). Cy attenuated the up-regulation of Snail induced by TGF-β in a dose-dependent manner with IC_{50} values of 22, 30, and 32 μM (Table 2) for pre-, co-, and post-treatment, respectively. Dp was more potent and inhibited the up-regulation of both fibronectin and Snail for the three different treatments with IC_{50} values ranging from 24 to 49 μM for fibronectin, and from 4 to 16.5 μM for Snail. Pg decreased the expression of Snail in pre- and co-treatment with IC_{50} values of 2.2 and 32 μM, respectively, and decreased the expression of fibronectin only in co-treatment with an IC_{50} value of 23 μM. Pt was effective at decreasing the up-regulation of Snail in pre- and co-treatment with an IC_{50} values of 9.5 and 22 μM, respectively. Finally, the inhibition of Twist expression by TGF-β was inversed by Cy in co-, and by Dp in post-treatment with concentrations of 35 and 25 μM, respectively (Figure 3B,C). Interestingly, Mv has no dose-response effect on the three EMT markers whether in pre-, co-, or post-treatment, even though we observed a light downward trend for Snail in co- and post-treatment (data not shown). Overall, Dp was the most potent inhibitor of TGF-β-induced EMT markers under pre-, co-, and post-treatment conditions.

The Impact of Anthocyanidins on TGF-β-Induced EMT Is Associated With an Inhibition of Smad2 and ERK Signaling Pathways in U-87 MG Cells

We next investigated whether anthocyanidins could modulate TGF-β-mediated Smad and non-Smad signaling pathways. Since Mv had no effect on EMT markers, we only tested the four other anthocyanidins under the same conditions as in Figure 3. Levels of phosphorylated and total Smad2, as well as phosphorylated and total ERK, which are associated with the TGF-β pathways [23], were analyzed by Western blotting (Figure 4). Compared to the stimulated control (cells treated with TGF-β only), the pre-treatment of U-87 MG cells with Cy, Dp, and Pt decreased the ratio of pSmad2/Smad2 in a dose-dependent manner with IC_{50} values of 44, 33.5, and 45 μM, respectively (Table 2). Co-treatment of U-87 MG cells with TGF-β and Cy or Dp significantly decreased Smad2 phosphorylation with an IC_{50} value being observed at concentrations of 43.5 and 24 μM, respectively (Table 2). When Dp was added after stimulation with TGF-β, it was able to attenuate the phosphorylation of Smad2 in a dose-dependant manner (Figure 4C). ERK phosphorylation was decreased by Dp in pre- and by Pg in post-treatment with IC_{50} values of 3 and 40 μM, respectively. These results indicate that anthocyanidins preferentially affect Smad2 and to a lesser

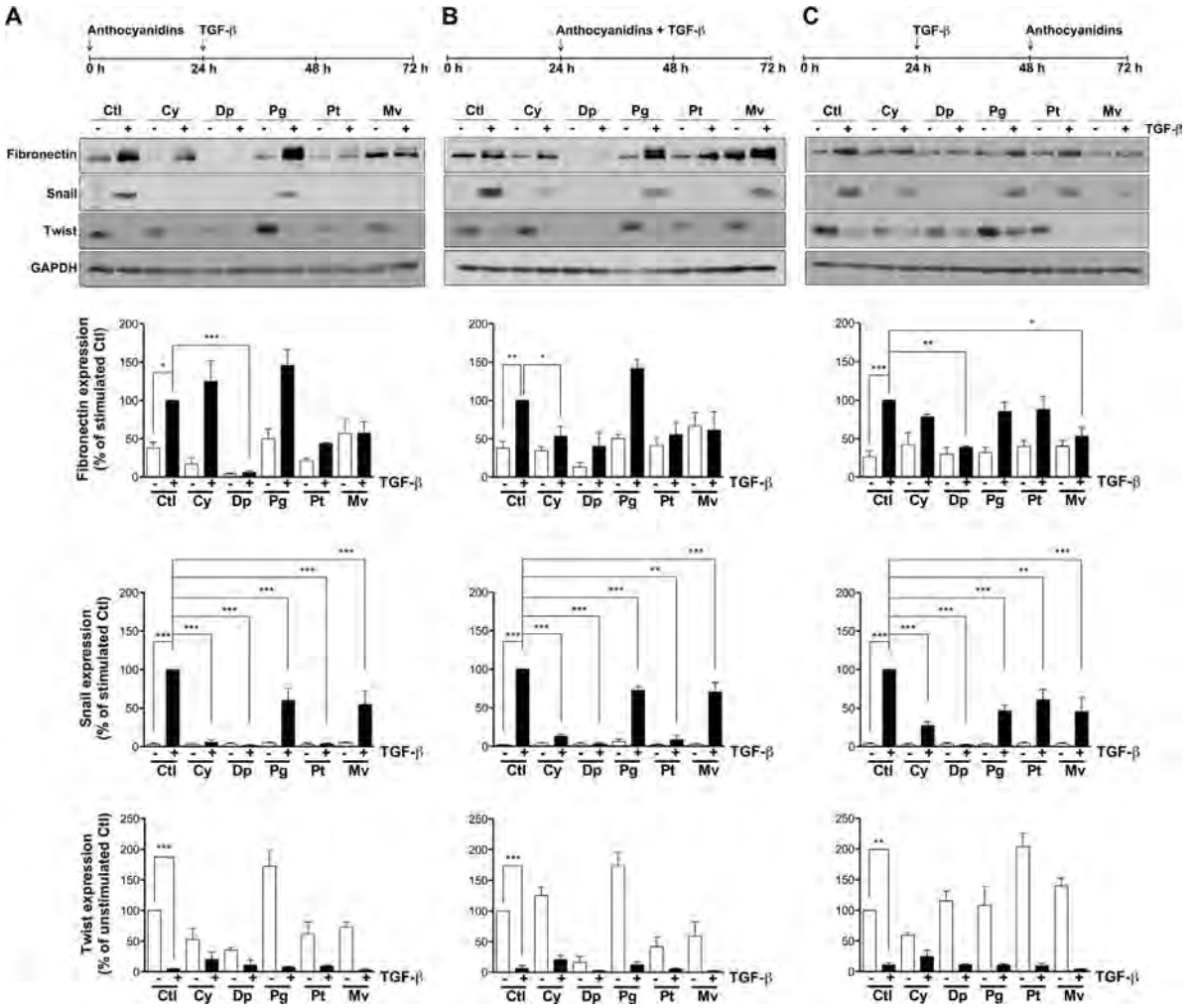

Figure 2. Pre-, co-, and post-treatment with anthocyanidins affects the changes in expression of EMT markers induced by TGF-β. U-87 MG cells were incubated in serum-free medium containing (or lacking) 50 μM of the indicated anthocyanidin. Cells were pre-treated with (A) anthocyanidins for 24 h, followed by TGF-β (10 ng/mL) for 48 h, or (B) serum starved for 24 h and co-treated with anthocyanidins and TGF-β for 48 h, or (C) serum starved for 24 h followed by the addition of TGF-β for 48 h and post-treated with anthocyanidins for the last 24 h. Cells were lysed and the expression levels of EMT markers monitored by immunoblotting using specific antibodies. The immunoreactive band intensities were analyzed by densitometry using ImageJ software and expressed in arbitrary units as a ratio of levels of marker proteins to housekeeping protein to correct for variations in the amount of protein loaded. The relative levels of proteins were also normalized to stimulated or unstimulated controls (value = 100%). Statistically significant differences were calculated by one-way ANOVA followed by Dunnett's test (*$P < 0.05$, **$P < 0.01$, and ***$P < 0.001$ vs. stimulated or unstimulated control). Data are representative of three or more independent experiments.

extend ERK signaling pathways associated with TGF-β induced EMT.

Anthocyanidins Inhibit TGF-β-Induced U-87 MG Cell Migration

During the process of EMT, U-87 MG cells adopt mesenchymal properties including increased migration activity [24]. In this part of the study, we evaluated the impact of anthocyanidins on cell migration. Prior to the cell migration assay, cells were treated with anthocyanidins at 25 μM in pre-, co-, and post-treatment with TGF-β. In order to discern the inhibitory action of each compound to one of the other, our rationale was based on the IC_{50} values obtained for the inhibition of EMT marker expression levels and of Smad- and non-Smad signaling pathways (Table 2) to choose this concentration. Upon treatment, cell migration was analyzed by the real-time system xCELLigence (Figure 5). TGF-β enhanced the migration of U-87 MG cells in a dose-dependent manner peaking at 10 ng/mL of TGF-β (Figure 5A). At higher concentrations of TGF-β (25–100 ng/mL), cell migration gradually decreased, reaching a basal level (Figure 5B). Incubation of cells using pre-, co-, or post-treatment with anthocyanidins significantly inhibited TGF-β-induced cell migration (Figure 5C). For each molecule, we next calculated inhibition percentages at $t = 4$ h under pre-, co-, and post-treatment conditions (Table 3). We found that Pt was the most potent molecule, inhibiting U-87 MG cell migration by

Table 1. Percentage Values of U-87 MG Cell Viability Monitored by Flow Cytometry After Treatment With Anthocyanidins (0, 35, and 50 μM)

		Anthocyanidin type of treatment		
	Anthocyanidin (μM)	Pre-treatment	Co-treatment	Post-treatment
Ctl (vehicle)	0	100.0	100.0	100.0
Cy	35	99.10 ± 0.20	99.10 ± 1.10	97.40 ± 9.00
	50	97.60 ± 1.70	93.80 ± 5.90	100.30 ± 4.90
Dp	35	92.60 ± 1.70	92.90 ± 9.60	100.70 ± 4.20
	50	78.50 ± 12.8	98.90 ± 2.00	99.50 ± 3.40
Pg	35	98.60 ± 0.40	97.00 ± 2.40	99.80 ± 6.70
	50	98.90 ± 1.70	98.60 ± 4.30	101.10 ± 4.70
Pt	35	100.30 ± 0.10	101.60 ± 0.40	103.00 ± 2.60
	50	99.00 ± 0.00	100.80 ± 1.40	96.80 ± 11.00
Mv	35	100.90 ± 0.40	102.90 ± 0.10	99.00 ± 7.90
	50	97.80 ± 2.00	103.60 ± 3.10	93.60 ± 15.70

Ouanouki et al. (2016).

73.3% and 42.6% in pre- and co-treatment, respectively. When post-treated with TGF-β, Pg showed the highest percentage of migratory inhibition (68%). Cy and Dp were also highly effective with 71.6% in pre- and 61.2% in post-treatment, respectively. Altogether, the results indicate that the inhibition of EMT by anthocyanidin (Cy, Dp, Pg, and Pt) treatment suppressed the ability of U-87 MG cells to adopt a mesenchymal behavior including migration.

DISCUSSION

In this study, we used U-87 MG cells as a model of grade IV glioblastoma in order to investigate the effects of five diet-derived anthocyanidins on TGF-β-mediated EMT. It is widely accepted that EMT is strongly involved in cancer cell invasion, dissemination, and metastasis [25], and that secretion of TGF-β by the tumor is a potent signaling factor to induce EMT [26]. Here, we confirm that, in response to TGF-β, U-87 MG cells lose their epithelial morphology and adopt a mesenchymal-like star-shaped morphology. The expression of three mesenchymal markers (fibronectin, Snail, Slug) increased while the expression of Twist decreased, correlating with mRNA transcript levels. These results were consistent with a previous study except that those authors demonstrated no effect of TGF-β on Twist expression according to their described treatment [27]. It should be noted that Twist is a transcriptional factor which is known to be up-regulated in glioma and to enhance cell invasion [6]. Also, it has been reported that the down-regulation of Twist triggers dissemination of tumor cells to proliferate and form metastases in a mouse model of squamous cell carcinoma [28]. Here, we demonstrate that Twist is expressed in U-87 MG cells, and that TGF-β down-regulated its expression. Although speculative, this mechanism may also be involved in U-87 MG cells. Under our experimental conditions, TGF-β reduced Twist expression and promoted a more invasive phenotype supporting epithelial–mesenchymal plasticity during tumor metastasis [28,29]. Thus, U-87 MG cells represent a suitable model of GBM for studying the pharmacological effects of anthocyanidins on EMT.

It is thought that the inhibition of TGF-β signaling leads to prevention of cancer metastasis through EMT inhibition. Accordingly, several TGF-β antagonists have been generated, such as TβRI inhibitors and monoclonal antibodies to TGF-β [12]. However, these antagonists represent an unsuitable option for patients because of their significant side effects and must therefore be optimized [10]. It is, however, possible to use these drugs in limited doses and in combination with other inhibitors that are more selective in targeting EMT [30]. Accordingly, we sought to examine the effects of diet-derived molecules such as anthocyanidins on EMT, and particularly the time of administration.

There is growing interest in dietary strategies to prevent and inhibit EMT [31]. Several studies have highlighted an important role for anthocyanidins as anti-carcinogenic, anti-diabetic, anti-aging, anti-oxidant, and anti-inflammatory molecules [32]. However, their effects on the EMT process remain unknown. We established three different treatment protocols in order to approximate conditions of EMT prevention (pre-treatment with anthocyanidins followed by exposure to TGF-β) or EMT inhibition (co- and post-treatment). Interestingly, all five anthocyanidins tested (Cy, Dp, Pg, Pt, and Mv) altered the expression of Snail whether used in pre-, co-, or post-treatment conditions. These results are in line with what is known about the anti-invasiveness effects of anthocyanins [33]. Indeed, Snail expression has been reported to be down-regulated by anthocyanins from *Vitis coignetiae* Pulliat in A549 lung cancer cells and in a human uterine cervical cancer HeLa cell model resulting in inhibition of invasion induced by EGF and TNF-α, respectively [21,34].

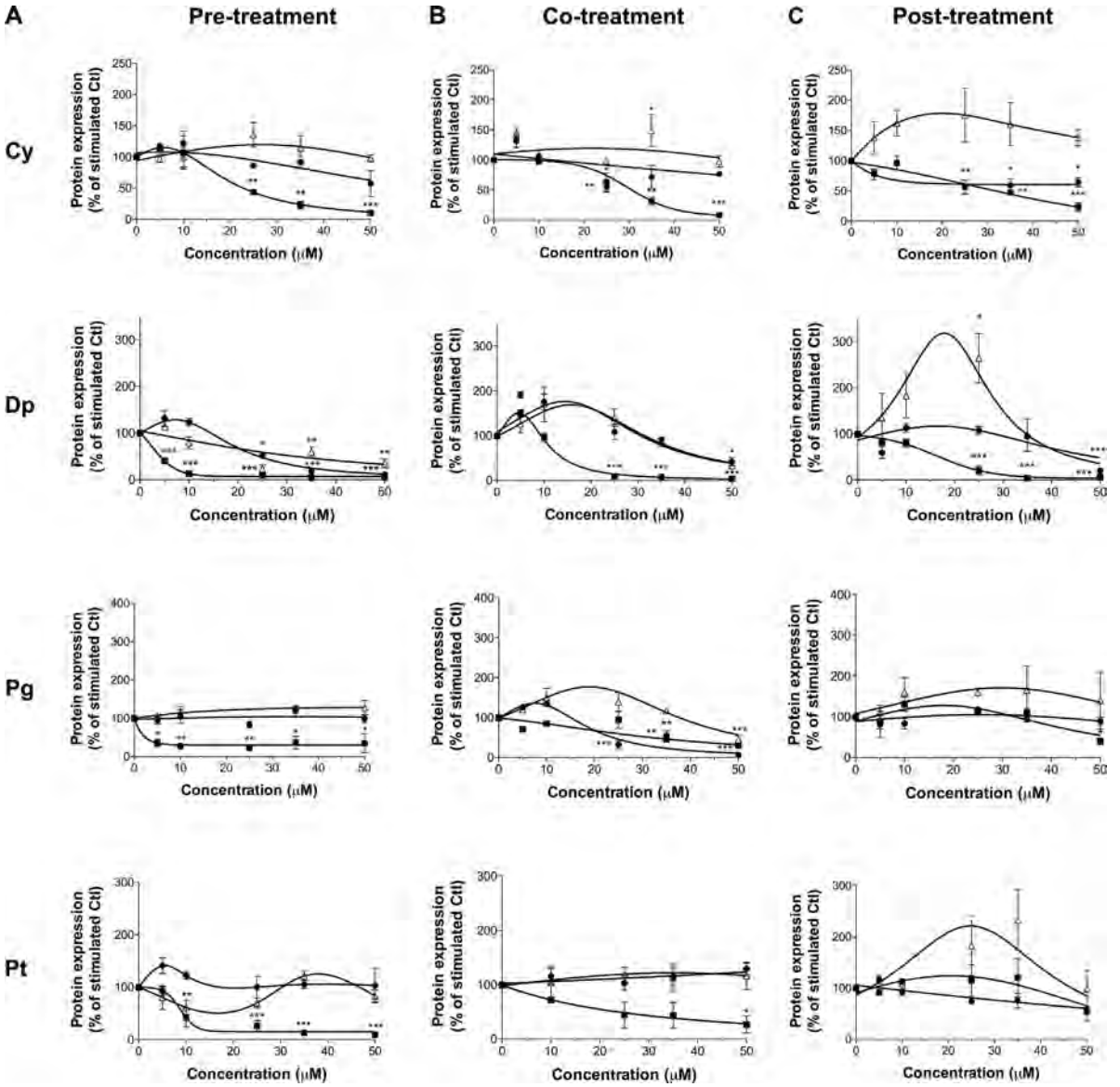

Figure 3. Anthocyanidins affect the TGF-β-induced changes in expression of EMT markers in a dose-dependent manner. U-87 MG cells were treated with various concentrations of each anthocyanidin in serum-free medium (A) prior to, (B) along with or (C) following addition of TGF-β (10 ng/mL). Cells were lysed and the protein expression levels of EMT markers monitored by immunoblotting using specific antibodies. ●fibronectin, ■Snail, △Twist. The immunoreactive band intensities were analyzed by densitometry using ImageJ software and expressed in arbitrary units as a ratio of levels of marker proteins to those of the housekeeping protein to correct for variation in the amount of protein loaded. The relative levels of proteins were also normalized to stimulated or unstimulated or control (value = 100%). Statistically significant differences were calculated by one-way ANOVA followed by Dunnett's test ($^{*}P < 0.05$, $^{**}P < 0.01$, and $^{***}P < 0.001$ vs. stimulated or unstimulated control). Data are representative of three or more independent experiments.

TGF-β can activate EMT in GBM via a Smad-dependent and a Smad-independent pathway [35]. The most important of these, the Smad2/3 pathway, plays a predominant role in TGF-β-induced EMT in glioblastoma cell lines [36]. Here, we have shown that Cy, Dp, Pg, and Pt attenuated TGF-β-induced phosphorylation of Smad2 in a dose-dependent manner. Dp was the most potent molecule with an IC_{50} as low as 12 μM when used in a post-treatment protocol with TGF-β and 24 μM under co-treatment conditions. This result supports a previous study which demonstrated that anthocyanins from purple corn inhibit TGF-β-induced Smad2 phosphorylation in mesangial cells [37].

The non-Smad signaling pathways mediated by TGF-β are also believed to be crucial in tumor progression [38] and were also assessed in this study. These include pathways such as ERK, JNK, and p38 MAPK [38]. Interestingly, TGF-β-mediated ERK phosphorylation was down-regulated in a dose dependant manner by Dp with an IC_{50} as low as 3 μM in pre-treatment. Pg also decreased ERK phosphorylation

Table 2. Comparative Overview of IC_{50} Values of Anthocyanidins on the Expression of EMT Markers and the TGF-β-Dependent Signaling Pathways

	Anthocyanidin type of treatment (IC_{50} in μM)		
	Pre-treatment	Co-treatment	Post-treatment
Cy			
Fibronectin	—	—	—
Snail	22.5	30	32
pSmad2	44	43.5	41
pERK	—	—	—
Dp			
Fibronectin	24	44	49
Snail	4	14	16.5
pSmad2	33.5	24	12.5
pERK	3	—	—
Pg			
Fibronectin	—	23.6	—
Snail	2.2	32	—
pSmad2	—	—	—
pERK	—	—	40
Pt			
Fibronectin	—	—	—
Snail	9.5	22	—
pSmad2	45	—	—
pERK	—	—	—

Ouanouki et al. (2016).

but less efficiently. We also looked at the JNK and p38 MAPK phosphorylations but none of the anthocyanidins tested inhibited them (data not shown). It has been reported that anthocyanins from black rice suppressed the non-Smad MAPK pathway RAS/RAF in the breast cancer cell line MDA-MB 453 resulting in metastasis inhibition [39]. Also, Dp was able to block the PI3K/AKT and MAPKs signal transduction cascades of human ovarian clear cell carcinoma (ES2) [40]. Our study therefore highlights the inhibitory effects of anthocyanidins in targeting both Smad2 and ERK signaling pathways.

We also investigated the effects of anthocyanidins on TGF-β-induced cell migration. It has been shown that Dp reduced the migration of human ovarian carcinoma cells (ES2) [40] and showed anti-invasive effects on HGF-mediated invasion in an MCF-10A breast cancer cell line [41]. Furthermore, Dp was shown to affect TGF-β-induced U-87 MG cell migration [42]. Here, we demonstrated that each anthocyanidin tested was able to alter U-87 MG cell migration, depending on the treatment protocol. More precisely, the anthocyanidin pre-treatment protocol showed better overall inhibition of TGF-β-induced U-87 MG cell migration for Cy and Pt, while Pg and Pt inhibition was seen with co-treatment conditions. Finally, Pg was the most potent migration inhibitor using post-treatment conditions. Depending on protocol treatment, there is a discrepancy between inhibitory action on EMT marker expression levels and that of cell migration by some anthocyanidins. For example, neither Pg nor Pt affected protein expression of fibronectin and Snail in post-treatment. However, these molecules were able to inhibit the migration of U-87 MG cells. This evidence indicates the existence of another potential inhibitory mechanism of action by which Pg and Pt alter TGF-β-induced EMT. Several key proteins play an important role in cell migration, such as proteins of the extracellular matrix (fibronectin, tenascin, collagen), integrins, cadherins or GTPases but also, migration can be induced by phosphorylation of kinases, such as, FAK, PYK2, PI3K, Smad, and ERK [43–46]. It is possible that the inhibition observed by these anthocyanidins is attributable to the inhibition of one or more of these key proteins involved in cell migration. Since Pg inhibited ERK phosphorylation in our assays, this could partially explain its inhibitory effect on cell migration. Moreover, it was reported that the JAK/Stat3 signaling pathway is also involved in cell migration and invasion of several cancer cell types [47] as well as in TGF-β-induced EMT in lung cancer cells [48]. It can therefore be envisioned that Pg and Pt may affect the JAK/Stat3 pathway regulating U-87 MG cell migration. It is noteworthy that the structure-function relationship of anthocyanidins may also be associated with their inhibitory action. It was reported that Dp exhibited the highest inhibitory potency in inhibiting migration of glioblastoma cells as compared with other anthocyanidins, this effect being related to ortho-dihydroxyphenyl structure on the B-ring and the presence of a free hydroxyl group at the position 3 [42]. Indeed, in light of our results, Dp showed a better inhibition of TGF-β-induced EMT in pre-, co-, and post-treatment followed by Cy, Pg, and Pt. Interestingly, Dp has three hydroxyl groups instead of two for Cy and Pt, and one for Pg in the B-ring. Additionally, Pt has also one methoxy group [49]. These observations suggest that the number of hydroxyl groups may confer a higher biological activity against TGF-β-induced EMT in our glioblastoma model.

We have done the first comparative study of anthocyanidin benefits using three different protocols: pre-, co-, and post-treatment with the EMT-inducer, TGF-β. The results show that whenever used before or after the induction of EMT, anthocyanidins are highly effective in inhibiting the EMT process. They significantly reversed the changes in the expression of mesenchymal markers induced by TGF-β, whether used to model cancer prevention or cancer treatment. This effect is associated with alterations in the TGF-β Smad and non-Smad signaling pathways, and is observed at low anthocyanidin concentrations. It is relevant to note that anthocyanin plasma concentrations are in the nM to low μM range [50–53], and that these molecules are able to cross the blood–brain barrier in vivo [54]. Thus, anthocyanidins could be promising pharmacologic agents for the prevention of cancer progression by affecting TGF-β-induced EMT. However, emerging issues concerning the role of synergy and the use of combinations of multiple anthocyanidins as natural

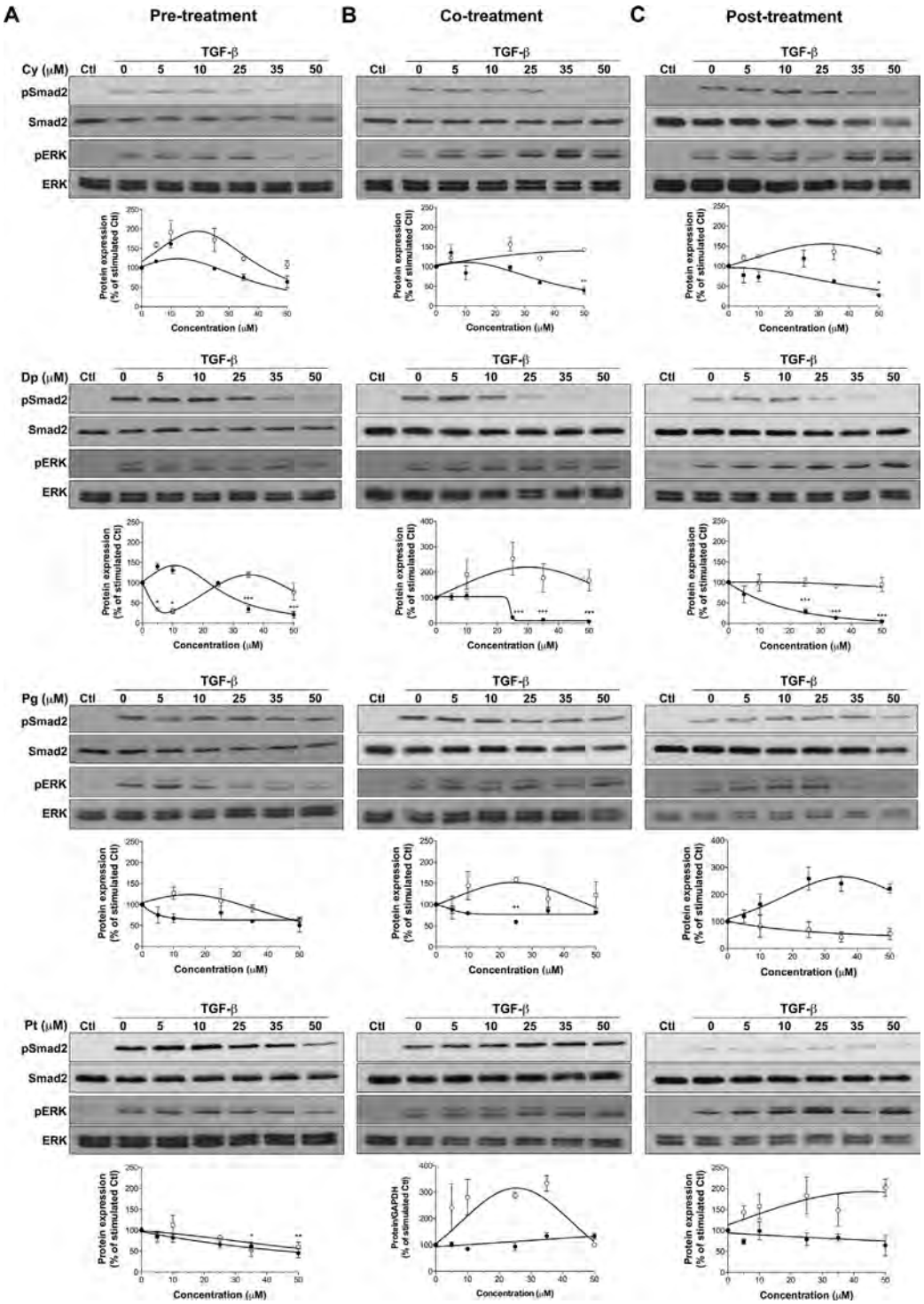

Figure 4. The impact of anthocyanidins on TGF-β-induced EMT in U-87 MG cells is associated with inhibition of the Smad2 and ERK signaling pathways. U-87 MG cells were treated with various concentrations of each anthocyanidin in (A) pre-, (B) co-, and (C) post-treatment with TGF-β (10 ng/mL). After these treatments, the levels of phosphorylated Smad2 and ERK, along with their respective total protein level, were monitored by immunoblotting using specific antibodies. ●pSmad2/Smad2, ○pERK/ERK. The immunoreactive band intensities were analyzed by densitometry using ImageJ software and expressed in arbitrary units as a ratio of levels of phosphorylated protein to those of the total protein to correct for variation in the amount of protein. The relative levels of phosphorylated protein were also normalized to the TGF-β stimulated control (value = 100%). Statistically significant differences were calculated by one-way ANOVA followed by Dunnett's test ($^{*}P < 0.05$, $^{**}P < 0.01$, and $^{***}P < 0.001$ vs. stimulated or unstimulated control). Data are representative of three or more independent experiments.

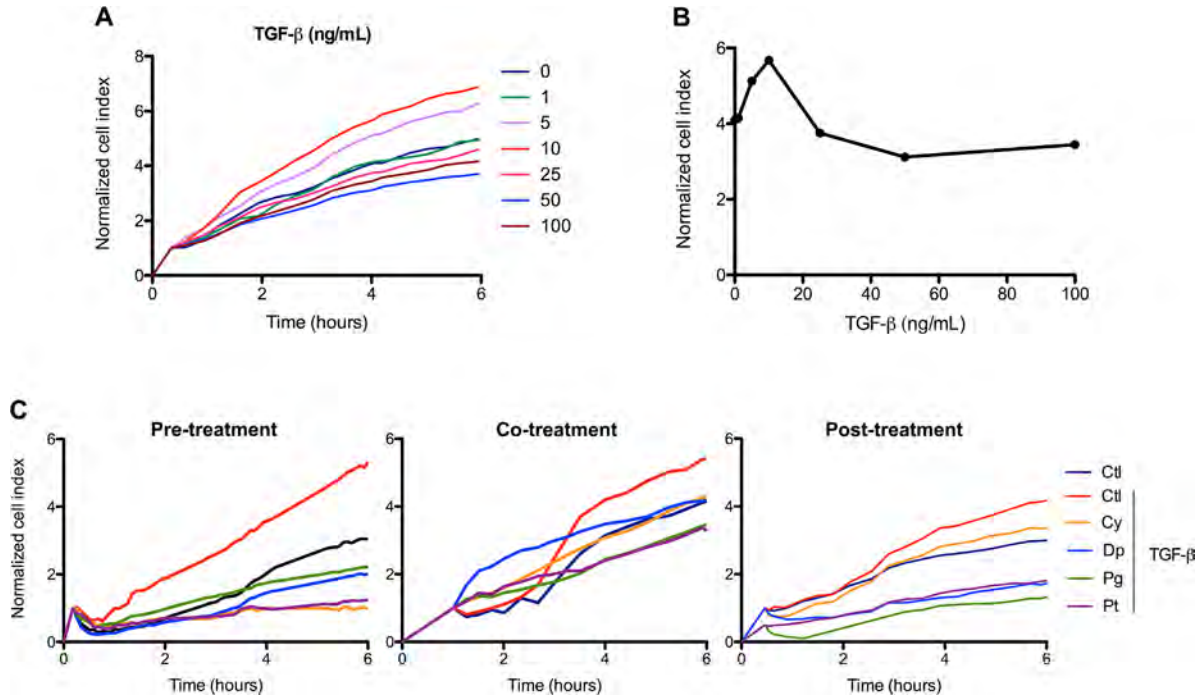

Figure 5. Anthocyanidins inhibit U-87 MG cell migration induced by TGF-β. U-87 MG cells were (A, B) pre-starved for 24 h and then treated with different concentrations of TGF-β for 48 h or (C) treated with anthocyanidins (25 μM) in pre-, co-, and post-treatment with TGF-β before adhesion onto CIM-Plates coated with 0.15% gelatin. (A, C) Impedance responses obtained from the xCELLigence system and (B) histogram representing TGF-β-induced migration of U-87 MG cells at 4 h, are shown. Values are means ± SEM of three independent experiments performed in quadruplicate. The normalized cell index at the base time is set to 1 in all wells.

Table 3. Percentage of U-87 MG Cell Migration Inhibition by Anthocyanidins in Pre-, Co- and Post-Treatment With TGF-β After 4 h of Migration on CIM-Plates

	Pre-treatment	Co-treatment	Post-treatment
Cy	71.6	26.7	16.4
Dp	58.3	16.7	61.2
Pg	50.5	41.7	68.0
Pt	73.3	42.6	57.3

Ouanouki et al. (2016).

chemopreventive compounds against GBM remain to be investigated.

ACKNOWLEDGMENT

A.O. is a *Fonds de Recherche Nature et technologies du Québec* (FRQNT) awardee. This study was funded by the Institutional Research Chair in Cancer Prevention and Treatment held by Dr. Borhane Annabi at UQAM.

REFERENCES

1. Campos B, Olsen LR, Urup T, Poulsen HS. A comprehensive profile of recurrent glioblastoma. Oncogene 2016 (in press).
2. Joo YN, Eun SY, Park SW, Lee JH, Chang KC, Kim HJ. Honokiol inhibits U87MG human glioblastoma cell invasion through endothelial cells by regulating membrane permeability and the epithelial-mesenchymal transition. Int J Oncol 2014;44: 187–194.
3. Stupp R, Mason WP, van den Bent MJ, et al. Radiotherapy plus concomitant and adjuvant temozolomide for glioblastoma. N Engl J Med 2005;352:987–996.
4. Lv S, Sun B, Dai C, et al. The downregulation of microRNA-146a modulates TGF-beta signaling pathways activity in glioblastoma. Mol Neurobiol 2015;52:1257–1262.
5. Vehlow A, Cordes N. Invasion as target for therapy of glioblastoma multiforme. Biochim Biophys Acta 2013;1836:236–244.
6. Mikheeva SA, Mikheev AM, Petit A, et al. TWIST1 promotes invasion through mesenchymal change in human glioblastoma. Mol Cancer 2010;9:194.
7. Kovacic JC, Mercader N, Torres M, Boehm M, Fuster V. Epithelial-to-mesenchymal and endothelial-to-mesenchymal transition: From cardiovascular development to disease. Circulation 2012;125:1795–1808.
8. Tiwari N, Gheldof A, Tatari M, Christofori G. EMT as the ultimate survival mechanism of cancer cells. Semin Cancer Biol 2012;22:194–207.
9. Kimura C, Hayashi M, Mizuno Y, Oike M. Endothelium-dependent epithelial-mesenchymal transition of tumor cells: Exclusive roles of transforming growth factor beta1 and beta2. Biochim Biophys Acta 2013;1830:4470–4481.
10. Wakefield LM, Roberts AB. TGF-beta signaling: Positive and negative effects on tumorigenesis. Curr Opin Genet Dev 2002;12:22–29.
11. Lee J, Choi JH, Joo CK. TGF-beta1 regulates cell fate during epithelial-mesenchymal transition by upregulating survivin. Cell Death Dis 2013;4:e714.
12. Miyazono K. Transforming growth factor-beta signaling in epithelial-mesenchymal transition and progression of cancer. Proc Jpn Acad Ser B Phys Biol Sci 2009;85:314–323.
13. Mayne ST, Playdon MC, Rock CL. Diet, nutrition, and cancer: Past, present and future. Nat Rev Clin Oncol 2016;13:504–515.

14. Lamy S, Akla N, Ouanouki A, Lord-Dufour S, Beliveau R. Diet-derived polyphenols inhibit angiogenesis by modulating the interleukin-6/STAT3 pathway. Exp Cell Res 2012;318:1586–1596.
15. Buchner FL, Bueno-de-Mesquita HB, Linseisen J, et al. Fruits and vegetables consumption and the risk of histological subtypes of lung cancer in the European Prospective Investigation into Cancer and Nutrition (EPIC). Cancer Causes Control 2010;21:357–371.
16. Russo M, Spagnuolo C, Tedesco I, Russo GL. Phytochemicals in cancer prevention and therapy: Truth or dare? Toxins 2010;2:517–551.
17. Zhang L, Wang X, Lai M. Modulation of epithelial-to-mesenchymal cancerous transition by natural products. Fitoterapia 2015;106:247–255.
18. Lamy S, Blanchette M, Michaud-Levesque J, et al. Delphinidin, a dietary anthocyanidin, inhibits vascular endothelial growth factor receptor-2 phosphorylation. Carcinogenesis 2006;27:989–996.
19. Hou DX. Potential mechanisms of cancer chemoprevention by anthocyanins. Curr Mol Med 2003;3:149–159.
20. Wang LS, Stoner GD. Anthocyanins and their role in cancer prevention. Cancer Lett 2008;269:281–290.
21. Lu JN, Lee WS, Kim MJ, et al. The inhibitory effect of anthocyanins on Akt on invasion and epithelial-mesenchymal transition is not associated with the anti-EGFR effect of the anthocyanins. Int J Oncol 2014;44:1756–1766.
22. Wang ZH, Zhang QS, Duan YL, Zhang JL, Li GF, Zheng DL. TGF-beta induced miR-132 enhances the activation of TGF-beta signaling through inhibiting SMAD7 expression in glioma cells. Biochem Biophys Res Commun 2015;463:187–192.
23. Attisano L, Wrana JL. Signal transduction by the TGF-beta superfamily. Science 2002;296:1646–1647.
24. Tso CL, Shintaku P, Chen J, et al. Primary glioblastomas express mesenchymal stem-like properties. Mol Cancer Res 2006;4:607–619.
25. Puisieux A, Brabletz T, Caramel J. Oncogenic roles of EMT-inducing transcription factors. Nat Cell Biol 2014;16:488–494.
26. Wendt MK, Allington TM, Schiemann WP. Mechanisms of the epithelial-mesenchymal transition by TGF-beta. Future Oncol 2009;5:1145–1168.
27. Joseph JV, Conroy S, Tomar T, et al. TGF-beta is an inducer of ZEB1-dependent mesenchymal transdifferentiation in glioblastoma that is associated with tumor invasion. Cell Death Dis 2014;5:e1443.
28. Tsai JH, Donaher JL, Murphy DA, Chau S, Yang J. Spatiotemporal regulation of epithelial-mesenchymal transition is essential for squamous cell carcinoma metastasis. Cancer Cell 2012;22:725–736.
29. Ocana OH, Corcoles R, Fabra A, et al. Metastatic colonization requires the repression of the epithelial-mesenchymal transition inducer Prrx1. Cancer Cell 2012;22:709–724.
30. Heldin CH, Vanlandewijck M, Moustakas A. Regulation of EMT by TGFbeta in cancer. FEBS Lett 2012;586:1959–1970.
31. Youdim KA, Dobbie MS, Kuhnle G, Proteggente AR, Abbott NJ, Rice-Evans C. Interaction between flavonoids and the blood-brain barrier: In vitro studies. J Neurochem 2003;85:180–192.
32. Rashid K, Wachira FN, Nyabuga JN, Wanyonyi B, Murilla G, Isaac AO. Kenyan purple tea anthocyanins ability to cross the blood brain barrier and reinforce brain antioxidant capacity in mice. Nutr Neurosci 2014;17:178–185.
33. Dreiseitel A, Oosterhuis B, Vukman KV, et al. Berry anthocyanins and anthocyanidins exhibit distinct affinities for the efflux transporters BCRP and MDR1. Br J Pharmacol 2009;158:1942–1950.
34. Lu JN, Lee WS, Yun JW, et al. Anthocyanins from vitis coignetiae pulliat inhibit cancer invasion and epithelial-mesenchymal transition, but these effects can be attenuated by tumor necrosis factor in human uterine cervical cancer HeLa cells. Evid Based Complement Alternat Med 2013;2013:503043.
35. Lv S, Zhang J, Han M, et al. Nucleolin promotes TGF-beta signaling initiation via TGF-beta receptor I in glioblastoma. J Mol Neurosci 2015;55:1–6.
36. Hu Y, Li J, Yan W, et al. Identifying novel glioma associated pathways based on systems biology level meta-analysis. BMC Syst Biol 2013;7:S9.
37. Li J, Lim SS, Lee JY, et al. Purple corn anthocyanins dampened high-glucose-induced mesangial fibrosis and inflammation: Possible renoprotective role in diabetic nephropathy. J Nutr Biochem 2012;23:320–331.
38. Derynck R, Muthusamy BP, Saeteurn KY. Signaling pathway cooperation in TGF-beta-induced epithelial-mesenchymal transition. Curr Opin Cell Biol 2014;31:56–66.
39. Chen XY, Zhou J, Luo LP, et al. Black rice anthocyanins suppress metastasis of breast cancer cells by targeting RAS/RAF/MAPK pathway. BioMed Res Int 2015;2015:414250.
40. Lim W, Jeong W, Song G. Delphinidin suppresses proliferation and migration of human ovarian clear cell carcinoma cells through blocking AKT and ERK1/2 MAPK signaling pathways. Mol Cell Endocrinol 2015;422:172–181.
41. Syed DN, Afaq F, Sarfaraz S, et al. Delphinidin inhibits cell proliferation and invasion via modulation of Met receptor phosphorylation. Toxicol Appl Pharmacol 2008;231:52–60.
42. Lamy S, Lafleur R, Bedard V, et al. Anthocyanidins inhibit migration of glioblastoma cells: Structure-activity relationship and involvement of the plasminolytic system. J Cell Biochem 2007;100:100–111.
43. Ridley AJ, Schwartz MA, Burridge K, et al. Cell migration: Integrating signals from front to back. Science 2003;302:1704–1709.
44. Demuth T, Berens ME. Molecular mechanisms of glioma cell migration and invasion. J Neurooncol 2004;70:217–228.
45. Huang C, Jacobson K, Schaller MD. MAP kinases and cell migration. J Cell Sci 2004;117:4619–4628.
46. Qiu X, Cheng JC, Zhao J, Chang HM, Leung PC. Transforming growth factor-beta stimulates human ovarian cancer cell migration by up-regulating connexin43 expression via Smad2/3 signaling. Cell Signal 2015;27:1956–1962.
47. Sansone P, Bromberg J. Targeting the interleukin-6/Jak/stat pathway in human malignancies. J Clin Oncol 2012;30:1005–1014.
48. Liu RY, Zeng Y, Lei Z, et al. JAK/STAT3 signaling is required for TGF-beta-induced epithelial-mesenchymal transition in lung cancer cells. Int J Oncol 2014;44:1643–1651.
49. Jing P, Bomser JA, Schwartz SJ, He J, Magnuson BA, Giusti MM. Structure-function relationships of anthocyanins from various anthocyanin-rich extracts on the inhibition of colon cancer cell growth. J Agric Food Chem 2008;56:9391–9398.
50. Marczylo TH, Cooke D, Brown K, Steward WP, Gescher AJ. Pharmacokinetics and metabolism of the putative cancer chemopreventive agent cyanidin-3-glucoside in mice. Cancer Chemother Pharmacol 2009;64:1261–1268.
51. Matsumoto H, Ichiyanagi T, Iida H, et al. Ingested delphinidin-3-rutinoside is primarily excreted to urine as the intact form and to bile as the methylated form in rats. J Agric Food Chem 2006;54:578–582.
52. Tsuda T, Horio F, Osawa T. Absorption and metabolism of cyanidin 3-O-beta-D-glucoside in rats. FEBS Lett 1999;449:179–182.
53. Wu X, Pittman HE, III, Prior RL. Pelargonidin is absorbed and metabolized differently than cyanidin after marionberry consumption in pigs. J Nutr 2004;134:2603–2610.
54. Andres-Lacueva C, Shukitt-Hale B, Galli RL, Jauregui O, Lamuela-Raventos RM, Joseph JA. Anthocyanins in aged blueberry-fed rats are found centrally and may enhance memory. Nutr Neurosci 2005;8:111–120.